

# **Lateral limiting pressure on square pile groups in undrained soil**

Brian B. Sheil<sup>1</sup> BE PhD

<sup>1</sup>Royal Academy of Engineering Research Fellow, Department of Engineering Science,  
University of Oxford, U.K.

Email: [brian.sheil@eng.ox.ac.uk](mailto:brian.sheil@eng.ox.ac.uk)

Initial submission, 16 May 2018

Revised submission, 30 October 2018

Revised submission, 15 October 2019

Main text word count: 2200

Tables: 1

Figures: 12

## **ABSTRACT**

In this paper, the lateral limiting pressure on square pile groups in undrained soil is explored using two-dimensional finite element modelling. A parametric study is conducted to assess the role of pile-soil adhesion, group size and pile spacing on group capacity and corresponding failure mechanisms. Results from the finite element output show that large groups of closely-spaced piles exhibit significant reductions in lateral capacity compared to equivalent single pile values. Significant variations in the load-sharing across the group are also observed, with the corner piles experiencing loads up to 162% above the group average for a 25-pile group. A simplified closed-form design approach is developed using a modified Ramberg-Osgood formulation to predict the lateral group capacity. The proposed approach is shown to provide excellent agreement to the numerical results and a rigorous upper bound prediction of a selection of field data and predictions determined using existing design guidelines.

## INTRODUCTION

Pile foundations are a commonly-adopted solution for supporting wind turbines, bridge piers, and high-rise buildings. Environmental phenomena such as wind, wave, and current induce significant lateral loads on these structures which in turn must be resisted by the foundation system. The behaviour of piled foundations subjected to lateral loads is potentially governed by both pile-soil-pile interaction and pile-soil-raft interaction. The design of free-standing pile groups and piled rafts necessitates rigorous consideration of ultimate load capacity, maximum settlement, differential settlement, and pile and raft moments and shears (Poulos 2001). In recent years, the focus of pile design has shifted from ultimate limit-state towards more economical serviceability limit-state (Sheil et al. 2018). As a result, the application of non-linear frameworks to pile groups has increased substantially over the last two decades. Within a non-linear framework, pile settlement is no longer uncoupled from the ultimate capacity and therefore an accurate estimation of capacity is a prerequisite for a rigorous analysis of the serviceability limit state.

The lateral capacity of a single pile in undrained soil has been the subject of a number of analytical (e.g. Murff & Hamilton, 1993), numerical (e.g. Brown & Shie, 1991; Yang & Jeremic, 2002), and experimental (e.g. Matlock 1970; Brown et al. 1988) investigations. Using the upper bound theory of plasticity, Murff and Hamilton (1993) noted that although the ultimate lateral resistance of a pile in undrained soil increased with depth, it eventually reached a limiting value at a ‘critical depth’. Below the critical depth, the limiting pressure corresponds to a plane strain ‘flow-around’ failure mechanism and depends exclusively on the pile-soil adhesion factor,  $\alpha$ . Solutions for this flow-around limiting pressure have been proposed by Randolph and Houlsby (1984), Murff et al. (1989) and Martin and Randolph (2006). The analysis of single piles subjected to lateral loads is commonly extended to that of pile groups through the use of ‘ $p$ -multipliers’. This involves factoring the capacity of each individual group pile to account for ‘group effects’. Brown et al. (1987) was one of the earliest studies to propose the use of  $p$ -multipliers which are typically defined as a function of the pile spacing in the direction of loading. Additional studies have explored the role of additional parameters on lateral group capacity including pile geometry and stiffness (Rao et al. 1998), group configuration (Chandrasekaran et al. 2010; Ilyas et al. 2004), ‘subgroups’ within the group (Zhou and Tokimatsu 2018), pile cap stiffness (Fayyazi et al. 2014), soil properties (Ashour and Ardalan 2011) and pile installation effects (Brown et al. 2001; Huang et al. 2001; Van Impe and Reese 2010).

Due to the associated expense, results from full-scale pile group load tests available in the public domain are limited (e.g. Brown et al. 1987; Meimon et al. 1986; Ruesta and Townsend 1997; Huang et al. 2001; Rollins and Sparks 2002; Snyder 2004; Rollins et al. 2006; Lemnitzer et al. 2010). Three-dimensional (e.g. Muqtadir and Desai 1986; Brown and Shie 1991; Kimura et al. 1995; Wakai et al. 1999; Zhang et al. 1999; Zhang and Small 2000; Yang and Jeremic 2003; Georgiadis 2014; Fayyazi et al. 2014) and two-dimensional (e.g. Bransby 1996; Bransby and Springman 1999) numerical investigations have greatly improved understanding of the effect of pile-soil-pile interaction on the limiting pressure of the surrounding soil. Using two-dimensional finite element (FE) modelling, Georgiadis et al. (2013a, 2013b) examined the limiting pressure of two side-by-side piles in undrained soil as well as the effect of the direction of loading. Similarly, Georgiadis et al. (2013c) considered a row of laterally loaded piles. More recently, Zhao et al. (2017a, 2017b) considered a tripod and tetrapod pile foundation in clay considering differences in both loading direction and pile-soil adhesion.

In this paper, two-dimensional FE modelling is used to explore the limiting resistance of square pile groups subjected to lateral loading. This study focuses on the maximum resistance that may develop along the length of the piles rather than its distribution with depth. The variables considered in the modelling include pile group size, pile spacing, and pile-soil adhesion. A modified Ramberg-Osgood analytical model is calibrated directly on the FE results and appraised against a selection of field data as well as predictions determined using existing design guidelines.

## FINITE ELEMENT MODEL

### *Geometry and material parameters*

In this study, a total of 420 displacement FE analyses were undertaken to explore the ultimate undrained lateral capacity of pile groups using the software programme Plaxis 2D Version 2016.1 (Brinkgreve et al. 2016). Plane strain conditions were adopted such that infinitely long piles are considered. The pile/soil parameters considered in this study are illustrated in Fig. 1 and listed in Table 1. Square pile groups were modelled using a pile diameter,  $D$ , of 1 m (fixed) and pile-to-pile spacing,  $s$  (varied). All piles were loaded by displacement control, with equal displacements to simulate rigid pile cap conditions; the potential for relative pile displacements to develop at some depth along the length of the piles is therefore not considered in this work. Lateral loading of a four-pile group in the direction shown in Fig. 1 was reported by Zhao et

al. (2017b) to produce the lowest ultimate capacity. In order to reduce the parameter space, this direction of loading was maintained in this study; the present results are therefore biased on the conservative side for alternative directions of loading.

The piles were modelled as a linear elastic steel pipe (Young's modulus = 210 GPa, Poisson's ratio = 0.1), with a wall thickness of 50 mm. The large wall thickness was to ensure the pile effectively behaved as a rigid body during loading. The soil was modelled as a weightless elastic-plastic Tresca material with an undrained shear strength,  $s_u = 100$  kPa, Poisson's ratio,  $\nu_u = 0.495$ , and Young's modulus,  $E_u = 500 \cdot s_u$ . Interface elements were introduced to consider the roughness at the pile-soil interface. The interface was also modelled as an elastic-plastic Tresca material with an undrained shear strength of  $\alpha \cdot s_u$ , shear stiffness of  $\sim 1$  MPa and normal stiffness of  $\sim 100$  MPa. These high interface stiffnesses are an attempt to simulate rigid-plastic interface behaviour. In this paper, the terms 'smooth' and 'rough' are used to denote values of  $\alpha$  of 0 and 1 respectively. Full tension interface conditions were imposed such that no gapping between pipe and soil was allowed in the modelling.

#### *Finite element mesh*

The soil was modelled using fourth-order, 15-node triangular elements while the steel pipe pile was modelled using 5-node beam elements. Exemplar meshes are shown in Fig. 2 for a single pile and pile group ( $n = 25$  chosen for illustrative purposes, where  $n$  is the number of piles in the group). The size of the computational domain (i.e. distances to external boundaries) varied depending on the number of piles in the group as well as the group spacing. The same mesh density was maintained in the region immediately surrounding the piles in all analyses, however. All boundaries were restricted from movement normal to their respective surface. Geometrical and loading symmetry was exploited in the modelling of the pile groups to reduce the number of elements used in the mesh.

#### *Extraction of individual pile reactions*

Plaxis provides an output of the total reaction force only rather than reactions for individual piles within the group. In order to obtain the individual pile reactions, a novel method of loading was necessary for this software package. A prescribed displacement was applied to a single point at the end of a 'dummy' beam which was in turn fixed to the pile structure collinear with the direction of loading (see Fig. 3). Since the pile was modelled as a pipe with an internal

cavity, the force generated by the prescribed displacement was fully transferred to the pipe structure through the dummy beam thereby allowing each individual pile force to be determined. The properties adopted for the steel pipe were also adopted for the dummy beam. Due to the high stiffness of the loading beam, relative displacements between piles were less than 0.1%. In all cases, the sum of the individual pile reactions were identical to the Plaxis output of the total reaction.

## *Verification*

The results of the modelling are presented in terms of a dimensionless bearing factor  $N_s = P/s_u D$  (for a single pile) or  $N_g = P/s_u Dn$  (for a pile group) where  $P$  is the total horizontal reaction per unit length. In Fig. 4 predictions of  $N_s$  determined using the present FE model are plotted against  $\alpha$ . Upper and lower bound plasticity predictions documented by Martin and Randolph (2006) and Randolph and Houlsby (1984) respectively are also superimposed on the plot. It can be seen that the present FE predictions show very good agreement to the plasticity solutions.

Figure 5 presents predictions of  $N_g$  for a two-pile group (loaded perpendicular to the pile-to-pile axis; Fig. 5(a)) and four-pile group (Fig. 5(b)), both plotted against normalised pile spacing,  $s/D$ . From Fig. 5(a), there is excellent agreement between the present results and predictions determined using the FE-based empirical equations reported by Georgiadis et al. (2013b). There is similarly excellent agreement between the present results and FE predictions documented by Zhao et al. (2017b) in Fig. 5(b).

## **FINITE ELEMENT RESULTS**

### *Ultimate bearing capacity*

The influence of group geometry (i.e.  $n$  and  $s/D$ ) on  $N_g$  is explored in Fig. 6 for both a rough ( $\alpha = 1$ ; Fig. 6(a)) and smooth ( $\alpha = 0$ ; Fig. 6(b)) pile-soil interface. It is also useful to consider these results in terms of a ‘group efficiency factor’,  $\eta = N_g/N_s$ , where a value of 1 indicates no ‘group effects’. Although values of  $s/D \lesssim 2.0$  are unlikely in practice (Mandolini and Viggiani 1997; Sheil et al. 2014, 2015), the trends presented in Fig. 6(a) show that closely-spaced pile groups experience significant reductions in  $N_g$ . An increase in  $n$  corresponds to additional reductions in  $N_g$  with corresponding values of  $\eta$  as low as 0.25 for  $n = 25$ . It can also be seen

that the normalised pile spacing required to achieve maximum efficiency ( $\eta = 1$ ) increases with group size e.g.  $\sim 5.25$  for  $n = 4$  and  $> 6$  for  $n = 25$ . Further, it is noticeable that the relationship between  $\eta$  and  $s/D$  is approximately linear for larger group sizes and for low values of  $s/D$ . To identify the cause of this linear relationship, the failure mechanisms corresponding to points (i) to (iv) marked on Fig. 6(a) are presented in Figs 7 and 8 for  $n = 4$  and 25 respectively. It can be seen that the highly nonlinear trends for  $n = 4$  is a result of distinct transitions in the failure mechanism from block failure (Fig. 7(a)) through to individual pile failure (Fig. 7(d)). By contrast, no clear transition between failure mechanisms is evident for the 25-pile group in Fig. 8. By comparison to the trends observed in Fig. 6(a), values of  $N_g$  plot lower for  $\alpha = 0$  in Fig. 6(b), as expected. However, values of  $\eta$  are generally notably higher while maximum efficiency is also achieved at lower values of  $s/D$ .

#### *Pile group load-sharing*

Pile group load-sharing is an important consideration for the structural design of the foundation to avoid overloading of individual piles. Figure 9 plots the variation of the bearing capacity factor for individual group piles (denoted  $N$ ) in the form of a percentage deviation from the group average ( $N_g$ ). In general, the results appear to be doubly-symmetric for these particular failure mechanisms (only the upper right quadrant is shown in Figs. 9(c) and 9(f) for clarity). Considering first a nine-pile group with rough interface conditions, it can be seen that the corner piles experience the greatest load for values of  $s/D$  up to  $\sim 2$  after which (the exterior) rows  $a$  and  $c$  experience approximately equal loads (see Fig. 9(a)). By contrast, (the centre) row  $b$  experiences significantly smaller loads due to a ‘shielding’ effect of the exterior piles. Comparing these results to those presented in Figs. 9(b) and 9(c) (for  $n = 16$  and 25 respectively), it can be seen that an increase in  $n$  induces significantly greater loads in row  $a$ . By way of example, for  $s/D = 3$  and rough interface the corner pile experiences a load that is 12%, 15%, and 21% above the group average for  $n = 9, 16$  and 25 respectively. Interestingly, comparing the left and right hand side of Fig. 9, the load-sharing trends appear to be near-independent of the interface roughness with one exception: the spacing required to achieve  $N = N_g$  is lower for a smooth interface, as observed in Fig. 6.

The spatial distribution of loads within  $n = 9$  and  $n = 25$  pile groups are shown in Fig. 10; only the upper right quadrant of the group is considered. The most apparent aspect of this plot is that the load distribution within the  $n = 9$  group is significantly more uniform than those

corresponding to the  $n = 25$  group. In particular, a remarkably non-uniform distribution can be seen for  $s/D = 2$  in Fig. 10(b). An increase in  $s/D$  from 2 to 4 results in a more uniform load distribution across rows 2 and 3 whereas row 1 is the last to ‘recover’.

## CLOSED-FORM ANALYTICAL APPROACH

For the development of a closed-form analytical approach, the well-established Ramberg–Osgood formulation has been adopted to describe the nonlinear relationship between  $N_g$  and  $s/D$  as follows:

$$s/D = \frac{\hat{N}}{a} + b \left( \frac{\hat{N}}{c \cdot N_s} \frac{n}{(n-1)} \right)^d \quad N_g \leq N_s \quad (1)$$

where  $a$ ,  $b$ ,  $c$  and  $d$  are empirical curve-fitting parameters and  $\hat{N}$  can be considered a transformed group capacity factor defined as follows:

$$\hat{N} = N_g - \frac{N_s}{n} \quad (2)$$

where  $N_s$  can be determined from lower bound plasticity theory (Randolph and Houlsby 1984):

$$N_s = \pi + 2\Delta + 2\cos(\Delta) + 4 \left[ \cos\left(\frac{\Delta}{2}\right) + \sin\left(\frac{\Delta}{2}\right) \right] \quad (3)$$

and  $\Delta = \sin^{-1}(\alpha)$ . All parameters have been determined using a least squares regression analysis on the FE data with the exception of parameter  $b$  (a constant value of 0.235 was adopted):

$$a = -0.069n + 4 \quad (4)$$

$$c = 0.0085n + 0.6715 \quad (5)$$

$$d = 0.217n + 5.758 \quad (6)$$

Predictions of  $\eta$  derived using Equation (1) are plotted against the present FE data in Fig. 11 where excellent agreement can be observed ( $R^2 = 0.995$ ).

## COMPARISONS TO FIELD DATA AND EXISTING DESIGN GUIDELINES

The proposed analytical approach provides a rigorous estimate of only the maximum resistance that may develop along the length of the piles. The assumption that this resistance is mobilised along the entire length of the piles therefore results in an upper-bound assessment of the overall group capacity. The variation of the group efficiency factor with group size predicted using the



present analytical model is plotted in Fig 12 for a rough pile-soil interface and a common pile spacing ( $s/D = 3$ ). Also superimposed on the plot are a selection of previously-documented field data as well as predictions determined using existing design guidelines (AASHTO, 2012; FEMA, 2012). The agreement between the field data and the design guidelines predictions are to be expected given the empirical nature of their development. It can be seen that the present analytical approach provides a good upper bound prediction of both the field data and the design guideline predictions. Further investigation of depth effects is clearly warranted for the development of an additional lower-bound predictive approach towards future application in practice.

## CONCLUSIONS

In this paper, a suite of 420 two-dimensional displacement FE analyses were conducted towards the development of a rigorous approach for the prediction of the maximum lateral limiting pressure on square pile groups in undrained soil. The main conclusions from the study are as follows:

- (a) The FE output showed that pile groups experience significant reductions in lateral capacity when piles are spaced closely together. This is exacerbated by an increase in group size.
- (b) It was observed that pile-soil roughness has a negligible influence on the group lateral limiting pressure if piles in large groups are spaced closely together ( $s/D \lesssim 4$ ).
- (c) The pile group load distributions exhibited increasing non-uniformity for larger group sizes and small pile spacings where the corner group piles consistently experienced the greatest loads.
- (d) A modified Ramberg-Osgood analytical model was developed for the prediction of the lateral capacity of the pile group based on the finite element results. The approach uses pile-soil adhesion, pile group size, and normalised pile spacing as inputs and showed excellent agreement to rigorous FE analyses.
- (e) Important assumptions that have been imposed in the modelling should be considered before applying the proposed approach in practice. The method provides a rigorous prediction of only the maximum resistance that may develop along the length of the piles. Assuming this resistance is mobilised along the entire length of the piles therefore provides an upper-bound assessment of the overall group capacity. In addition, the

development of differential displacements between piles with depth may lead to slight alterations in the group interactions.

## ACKNOWLEDGEMENTS

The author is supported by the Royal Academy of Engineering under the Research Fellowship scheme.

## REFERENCES

- Ashour, M. and Ardalan, H., 2011. Employment of the  $p$ -multiplier in pile-group analysis. *Journal of bridge engineering*, 16(5), pp.612-623.
- AASHTO, 2012. "AASHTO LRFD bridge design specifications", Washington, DC.
- Bransby, M.F., 1996. Difference between load-transfer relationships for laterally loaded pile groups: Active  $p$ - $y$  or passive  $p$ - $\delta$ . *Journal of geotechnical engineering*, 122(12), pp.1015-1018.
- Bransby, M.F. and Springman, S., 1999. Selection of load-transfer functions for passive lateral loading of pile groups. *Computers and Geotechnics*, 24(3), pp.155-184.
- Brinkgreve, R.B.J., Kumarswamy, S. and Swolfs, W.M., 2016. PLAXIS 2-D Version 2016. *PLAXIS bv, The Netherlands*.
- Brown, D.A., Reese, L.C. and O'Neill, M.W., 1987. Cyclic lateral loading of a large-scale pile group. *Journal of Geotechnical Engineering*, 113(11), pp.1326-1343.
- Brown, D.A., Morrison, C. and Reese, L.C., 1988. Lateral load behaviour of pile group in sand. *Journal of Geotechnical Engineering*, 114(11), pp.1261-1276.
- Brown, D.A. and Shie, C.F., 1991. Some numerical experiments with a three dimensional finite element model of a laterally loaded pile. *Computers and Geotechnics*, 12(2), pp.149-162.
- Brown, D. A., O'Neill, M. W., Hoit, M., McVay, M., EL Naggar, M. H., and Chakraborty, S. (2001). "Static and dynamic lateral loading of pile groups." Rep. No. NCHRP 461, National Cooperative Highway Research Program, Transportation Research Board, Washington, DC.
- Chandrasekaran, S.S., Boominathan, A. and Dodagoudar, G.R., 2009. Group interaction effects on laterally loaded piles in clay. *Journal of Geotechnical and Geoenvironmental Engineering*, 136(4), pp.573-582.
- Fayyazi, M.S., Taiebat, M. and Liam Finn, W.D. 2014 Group reduction factors for analysis of laterally loaded pile groups. *Canadian Geotechnical Journal*, 51(7), pp.758-769.
- FEMA, 2012. "Foundation analysis and design", FEMA P-751, Washington, DC.
- Georgiadis, K., 2014. Variation of limiting lateral soil pressure with depth for pile rows in clay. *Computers and Geotechnics*, 62, pp.164-174.
- Georgiadis, K., Sloan, S.W. and Lyamin, A.V., 2013a. Effect of loading direction on the ultimate lateral soil pressure of two piles in clay. *Géotechnique*, 63(13), p.1170.
- Georgiadis, K., Sloan, S.W. and Lyamin, A.V., 2013b. Ultimate lateral pressure of two side-by-side piles in clay. *Géotechnique*, 63(9), p.733.

- Georgiadis, K., Sloan, S.W. and Lyamin, A.V., 2013c. Undrained limiting lateral soil pressure on a row of piles. *Computers and Geotechnics*, 54, pp.175–184.
- Huang, A.B., Hsueh, C.K., O'Neill, M.W., Chern, S. and Chen, C., 2001. Effects of construction on laterally loaded pile groups. *Journal of Geotechnical and Geoenvironmental Engineering*, 127(5), pp.385–397.
- Ilyas, T., Leung, C.F., Chow, Y.K. and Budi, S.S. 2004 Centrifuge model study of laterally loaded pile groups in clay. *Journal of Geotechnical and Geoenvironmental Engineering*, 130(3), pp.274–283.
- Kimura, M., Adachi, T., Kamei, H. and Zhang, F., 1995. 3D Finite Element Analyses of the Ultimate Behavior of Laterally Loaded Cast-in-place Concrete Piles. 15<sup>th</sup> International Conference of Numerical Models in Geomechanics, Davos, Switzerland, 589–594.
- Lemnitzer, A., Khalili-Tehrani, P., Ahlberg, E.R., Rha, C., Taciroglu, E., Wallace, J.W. and Stewart, J.P., 2010. Nonlinear efficiency of bored pile group under lateral loading. *Journal of Geotechnical and Geoenvironmental engineering*, 136(12), pp.1673–1685.
- Mandolini, A. and Viggiani, C., 1997. Settlement of piled foundations. *Géotechnique*, 47(4), pp.791–816.
- Martin, C.M. and Randolph, M.F., 2006. Upper-bound analysis of lateral pile capacity in cohesive soil. *Géotechnique*, 56(2), pp.141–145.
- Matlock, H., 1970. Correlations for design of laterally loaded piles in soft clay. Offshore technology in civil engineering's hall of fame papers from the early years, pp.77–94.
- Meimon, Y., Baguelin, F. and Jezequel, J.F., 1986, May. Pile group behaviour under long time lateral monotonic and cyclic loading. In Proceedings, Third International Conference on Numerical Methods in Offshore Piling, Inst. Francais du Petrole, Nantes, France (pp. 285–302).
- Muqtadir, A. and Desai, C.S., 1986. Three-dimensional analysis of a pile-group foundation. *International Journal for Numerical and Analytical Methods in Geomechanics*, 10(1), pp.41–58.
- Murff, J.D. and Hamilton, J.M., 1993. P-ultimate for undrained analysis of laterally loaded piles. *Journal of Geotechnical Engineering*, 119(1), pp.91–107.
- Murff, J.D., Wagner, D.A. and Randolph, M.F., 1989. Pipe penetration in cohesive soil. *Géotechnique*, 39(2), pp.213–229.
- Poulos, H.G., 2001. Piled raft foundations: design and applications. *Geotechnique*, 51(2), pp.95–113.
- Randolph, M.F. and Houlsby, G.T., 1984. The limiting pressure on a circular pile loaded laterally in cohesive soil. *Geotechnique*, 34(4), pp.613–623.
- Rao, S.N., Ramakrishna, V.G.S.T. and Rao, M.B., 1998. Influence of rigidity on laterally loaded pile groups in marine clay. *Journal of Geotechnical and Geoenvironmental Engineering*, 124(6), pp.542–549.
- Rollins, K.M., Peterson, K.T. and Weaver, T.J., 1998. Lateral load behaviour of full-scale pile group in clay. *Journal of Geotechnical and Geoenvironmental Engineering*, 124(6), pp.468–478.
- Rollins, K.M. and Sparks, A., 2002. Lateral resistance of full-scale pile cap with gravel backfill. *Journal of Geotechnical and Geoenvironmental Engineering*, 128(9), pp.711–723.
- Rollins, K.M., Olsen, K.G., Jensen, D.H., Garrett, B.H., Olsen, R.J. and Egbert, J.J., 2006. Pile spacing effects on lateral pile group behaviour: Analysis. *Journal of geotechnical and geoenvironmental engineering*, 132(10), pp.1272–1283.

- Ruesta, P.F. and Townsend, F.C., 1997. Evaluation of laterally loaded pile group at Roosevelt Bridge. *Journal of Geotechnical and Geoenvironmental Engineering*, 123(12), pp.1153–1161.
- Sheil, B.B. and McCabe, B.A., 2014. A finite element–based approach for predictions of rigid pile group stiffness efficiency in clays. *Acta Geotechnica*, 9(3), pp.469–484.
- Sheil, B.B. and McCabe, B.A., 2015. Numerical modelling of pile foundation angular distortion. *Soils and Foundations*, 55(3), pp.614–625.
- Sheil, B.B., McCabe, B.A., Comodromos, E.M. and Lehane, B.M., 2018. Pile groups under axial loading: an appraisal of simplified non-linear prediction models. *Géotechnique*, pp.1-15.
- Snyder, J.L. 2004 “Full-scale lateral-load tests of a 3x5 pile group in soft clays and silts”. Master of Science thesis, Department of Civil and Environmental Engineering, Brigham Young University.
- Taghavi, A. and Muraleetharan, K.K., 2016. Analysis of laterally loaded pile groups in improved soft clay. *International Journal of Geomechanics*, 17(4), 04016098.
- Van Impe, W.F. and Reese, L.C., 2010. *Single piles and pile groups under lateral loading*. CRC press.
- Wakai, A., Gose, S. and Ugai, K., 1999. 3–D elasto–plastic finite element analyses of pile foundations subjected to lateral loading. *Soils and Foundations*, 39(1), pp.97–111.
- Yang, Z. & Jeremic, B. (2002). Numerical analysis of pile behaviour under lateral loads in layered elastic–plastic soils. *Int. J. Numer. Anal. Methods Geomech.* 26, pp.1385–1406.
- Yang, Z. and Jeremić, B., 2003. Numerical study of group effects for pile groups in sands. *International Journal for Numerical and Analytical Methods in Geomechanics*, 27(15), pp.1255–1276.
- Zhang, L., McVay, M.C. and Lai, P., 1999. Numerical analysis of laterally loaded 3× 3 to 7× 3 pile groups in sands. *Journal of Geotechnical and Geoenvironmental Engineering*, 125(11), pp.936-946.
- Zhang, H.H. and Small, J.C., 2000. Analysis of capped pile groups subjected to horizontal and vertical loads. *Computers and Geotechnics*, 26(1), pp.1-21.
- Zhao, Z., Kouretzis, G., Sloan, S. and Gao, Y., 2017a. Ultimate lateral resistance of tripod pile foundation in clay. *Computers and Geotechnics*, 92, pp.220–228.
- Zhao, Z., Li, D., Zhang, F. and Qiu, Y., 2017b. Ultimate lateral bearing capacity of tetrapod jacket foundation in clay. *Computers and Geotechnics*, 84, pp.164–173.
- Zhou, Y. and Tokimatsu, K., 2018. Numerical evaluation of pile group effect of a composite group. *Soils and Foundations*. [https:// doi.org/10.1016/j.sandf.2018.04.004](https://doi.org/10.1016/j.sandf.2018.04.004)

353 **NOTATION LIST**

354	$a, b, c, d$	Empirical curve-fitting parameters
355	$D$	Pile diameter
356	$E_u$	Undrained Young's modulus of the soil
357	$n$	Pile group size
358	$N$	Dimensionless bearing factor for individual group piles
359	$N_s$	Dimensionless bearing factor for a single pile
360	$N_g$	Dimensionless bearing factor for a pile group
361	$\hat{N}$	Transformed dimensionless bearing factor
362	$P$	Total horizontal reaction per unit length
363	$s$	Pile-to-pile spacing
364	$s_u$	Undrained shear strength of the soil
365	$\alpha$	Interface roughness factor
366	$\delta$	Pile displacement
367	$\eta$	Pile group efficiency factor
368	$\nu_u$	Undrained Poisson's ratio of the soil
369		

**Table 1** Pile/soil parameters considered in the modelling

Parameter	Value
Pile diameter, $D$ (m)	1.0
Group size, $n$	$2^2, 3^2, 4^2, 5^2$
Normalised pile spacing, $s/D$	1.0 to 6.0 in increments of 0.25
Pile–soil adhesion factor, $\alpha$	0, 0.25, 0.5, 0.75, 1.0

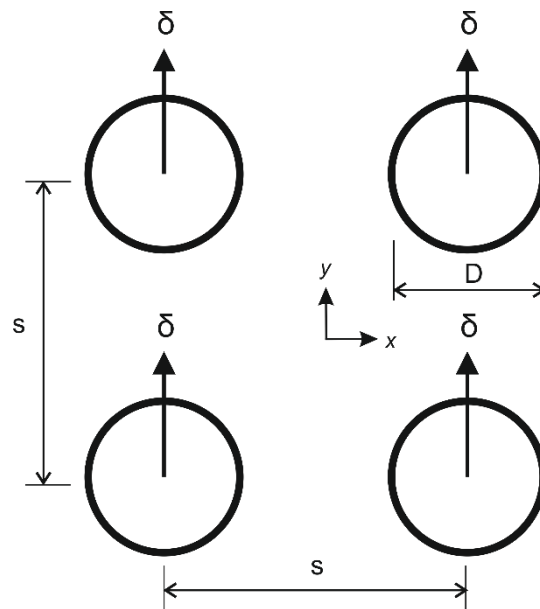


**Fig. 1** Problem definition (four-pile group shown for illustrative purposes)

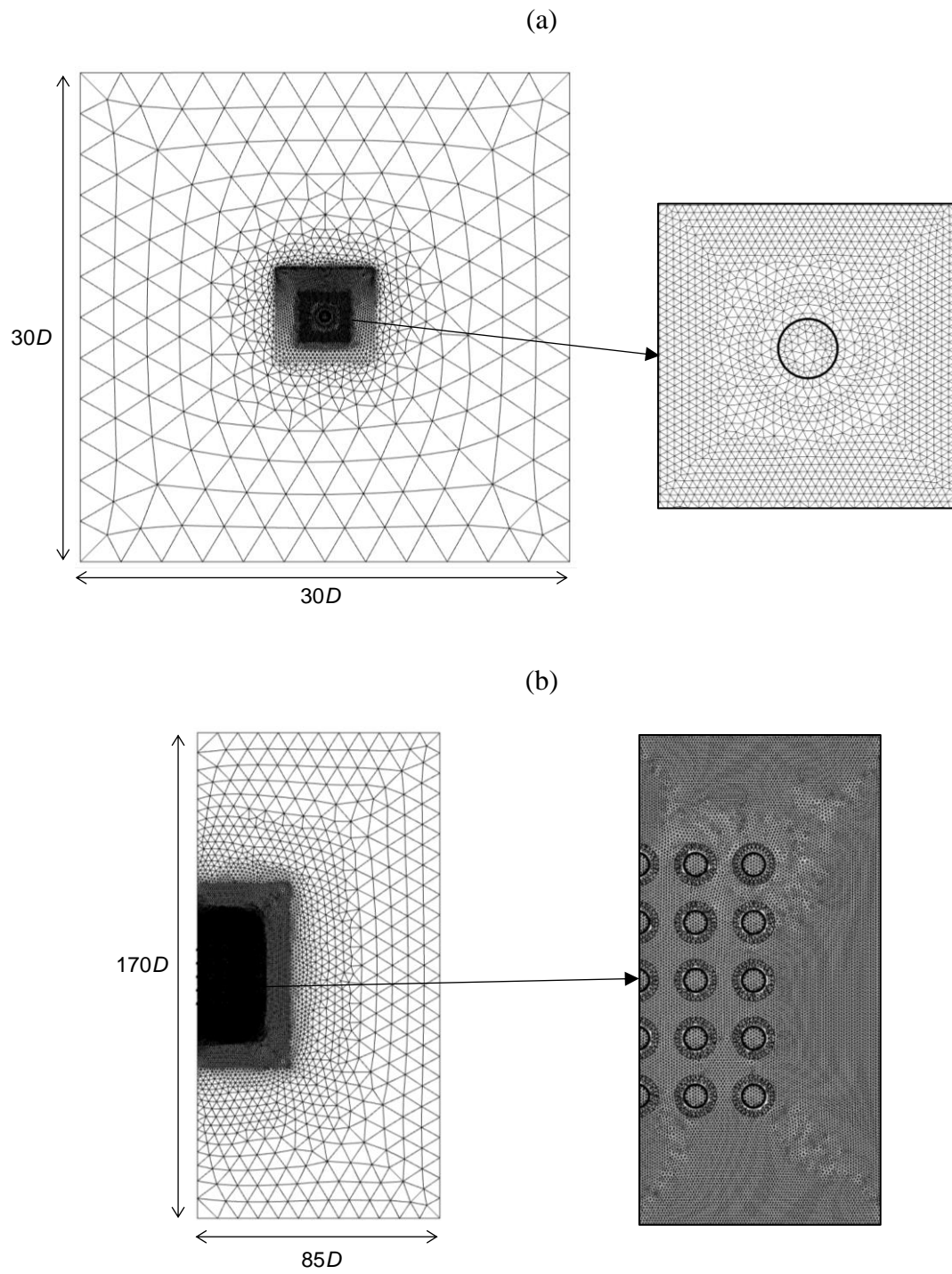


**Fig. 2** Exemplar finite element meshes: (a) single pile ( $\sim 7700$  elements), (b) pile group ( $n = 25$ ,  $s/D = 2.5$ ,  $\sim 50,000$  elements)

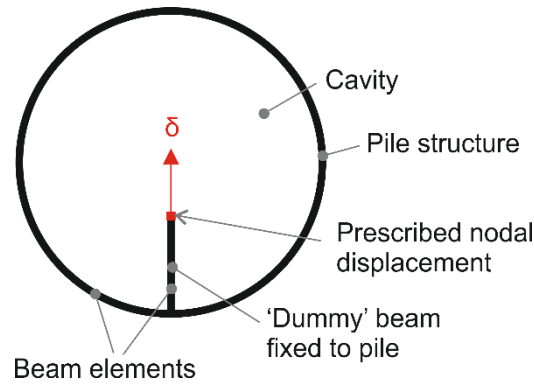


**Fig. 3** Individual pile load extraction using ‘dummy’ beam elements fixed to pile structure collinear with the direction of loading

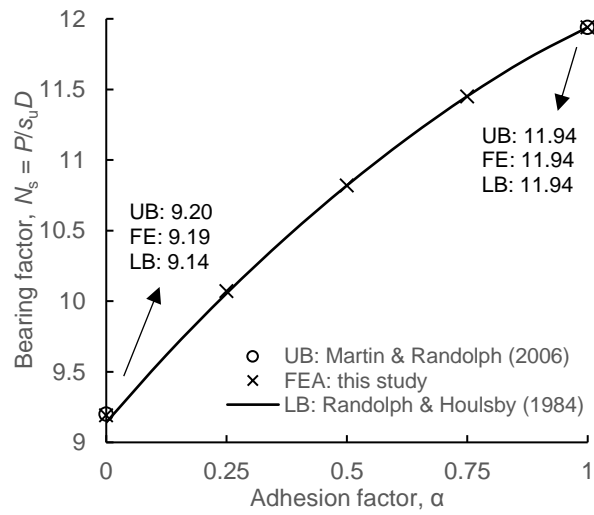


**Fig. 4** Validation of present FE predictions of single pile bearing capacity for the full range of adhesion factors through comparisons to Randolph and Houlsby (1984) and Martin and Randolph (2006) solutions



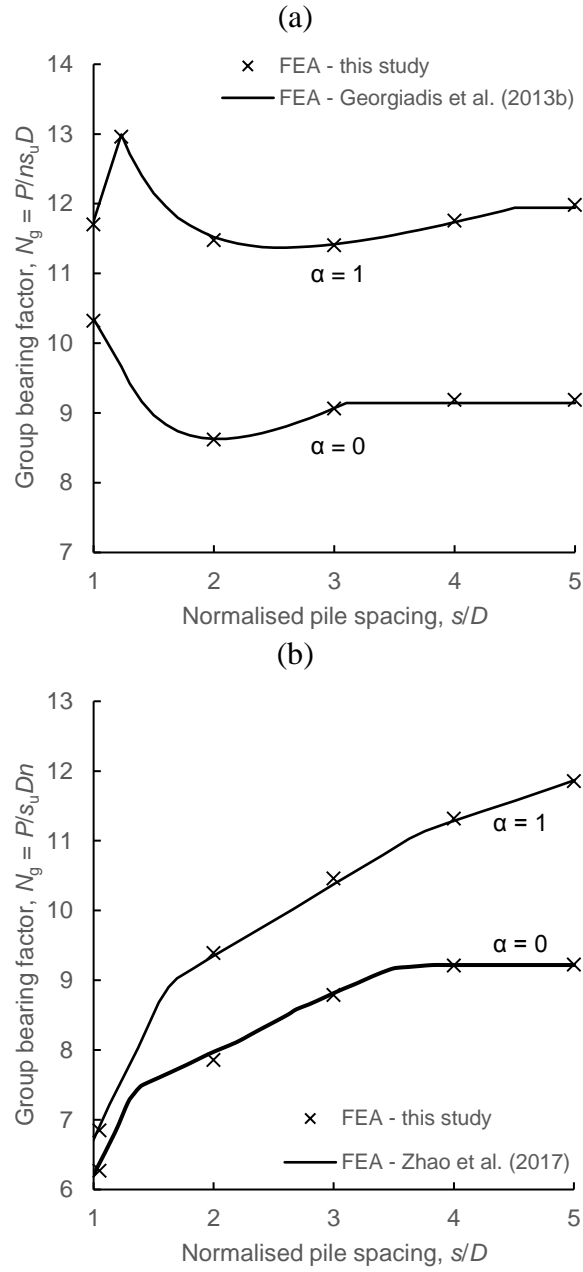


**Fig. 5** Validation of present FE predictions of pile group bearing capacity for a variation in pile spacing through comparisons to Georgiadis et al. (2013b) and Zhao et al. (2017) predictions: (a)  $n = 2^a$ , (b)  $n = 4$

<sup>a</sup>In this instance loading is perpendicular to pile-to-pile axis

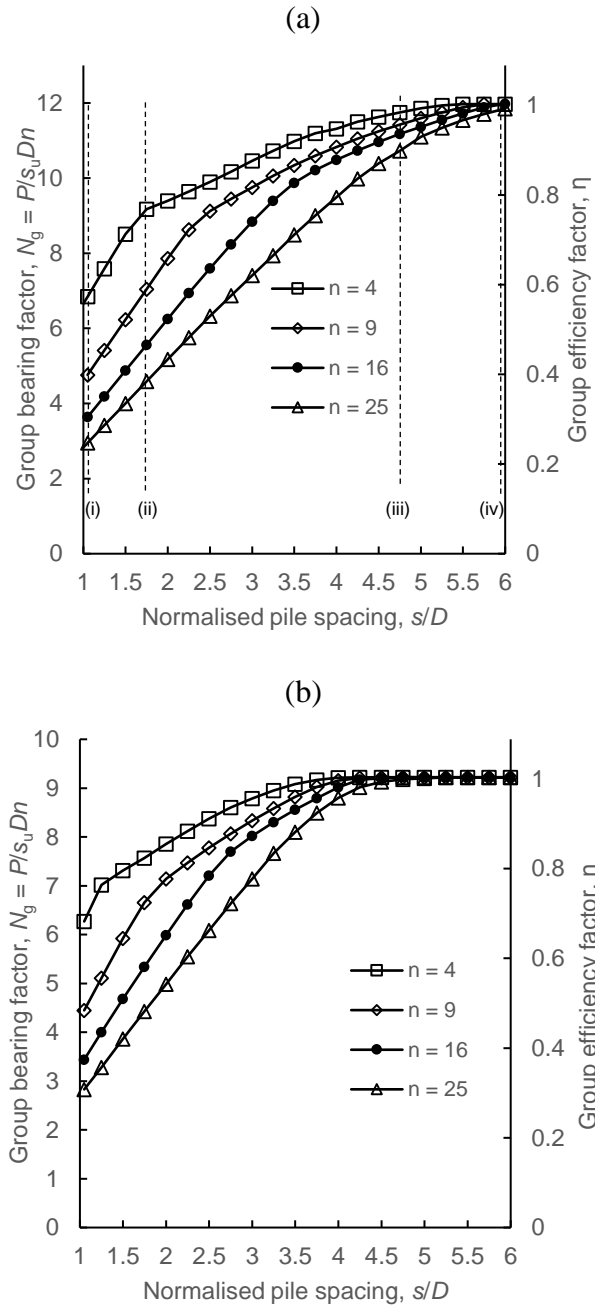


**Fig. 6** FE-predicted influence of pile group size and spacing on ultimate group capacity: (a) rough interface ( $\alpha = 1$ ), (b) smooth interface ( $\alpha = 0$ )

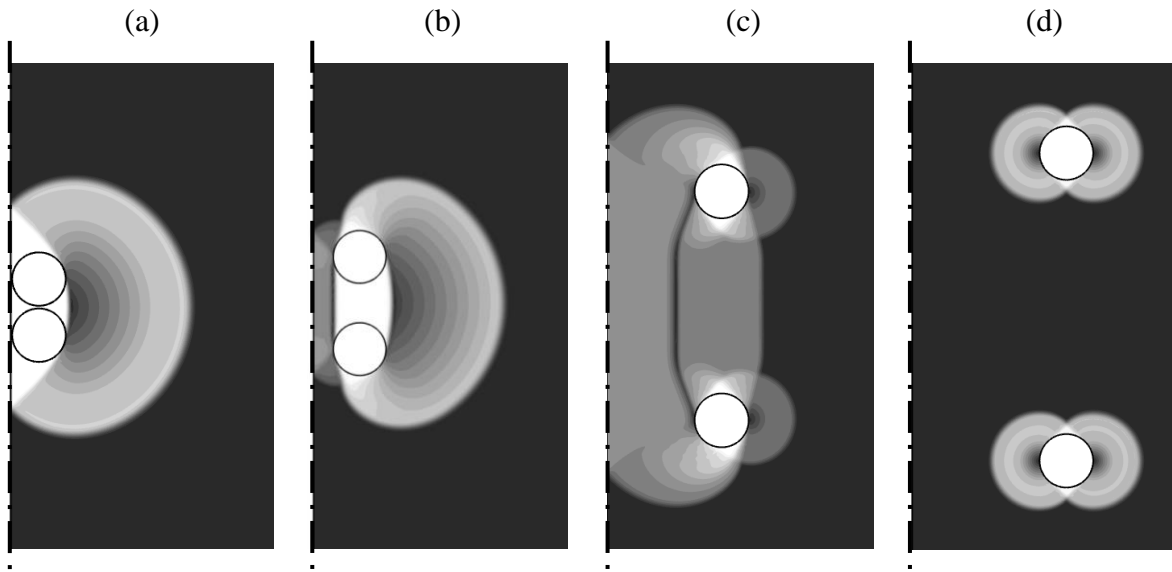


**Fig. 7** FE-predicted incremental soil displacements showing failure mechanisms for  $n = 4$  group with rough interface: (a)  $s/D = 1.05$ , (b)  $s/D = 1.75$ , (c)  $s/D = 4.5$ , (d)  $s/D = 6$

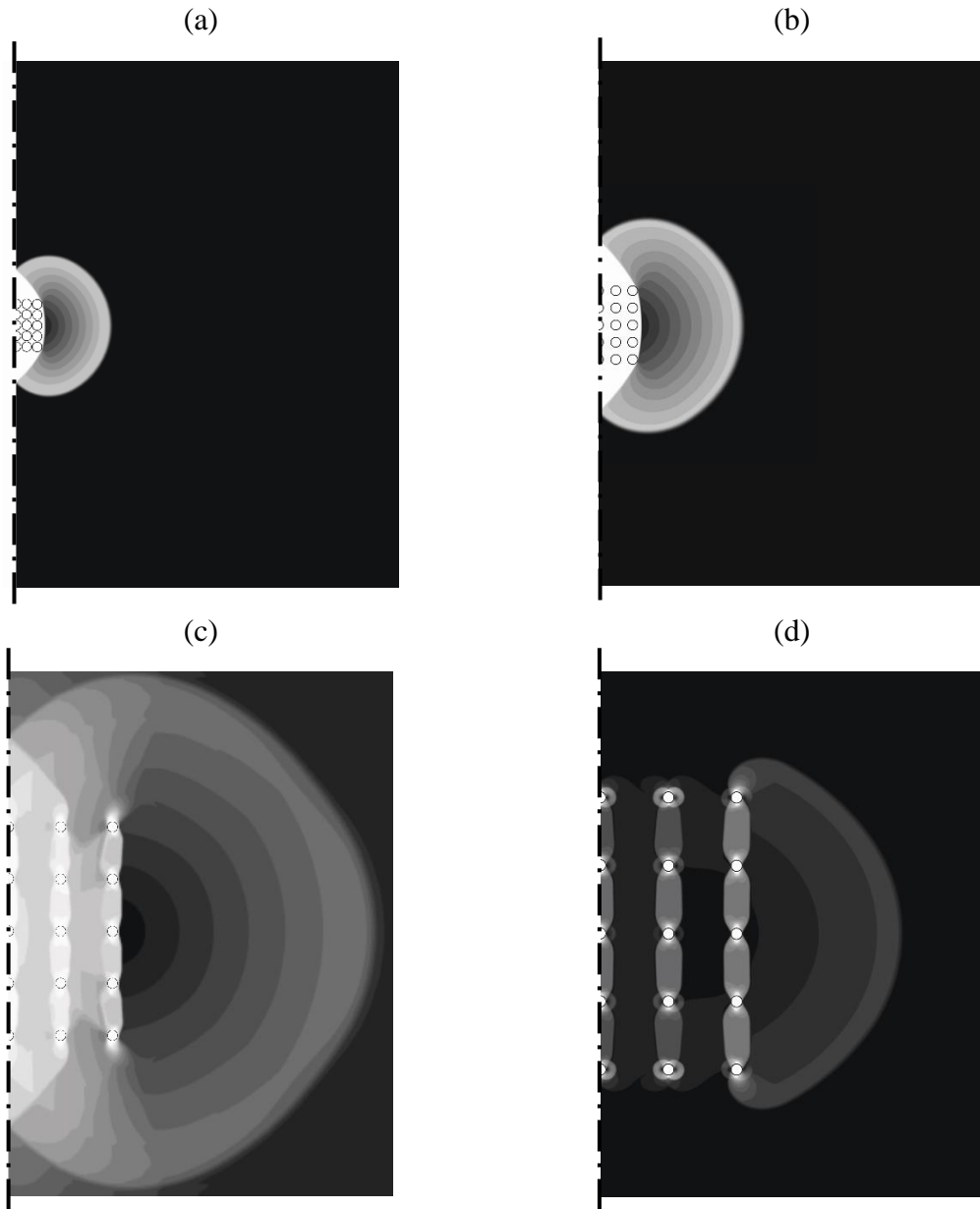


**Fig. 8** FE-predicted incremental soil displacements showing failure mechanisms for  $n = 25$  group with rough interface: (a)  $s/D = 1.05$ , (b)  $s/D = 1.75$ , (c)  $s/D = 4.5$ , (d)  $s/D = 6$

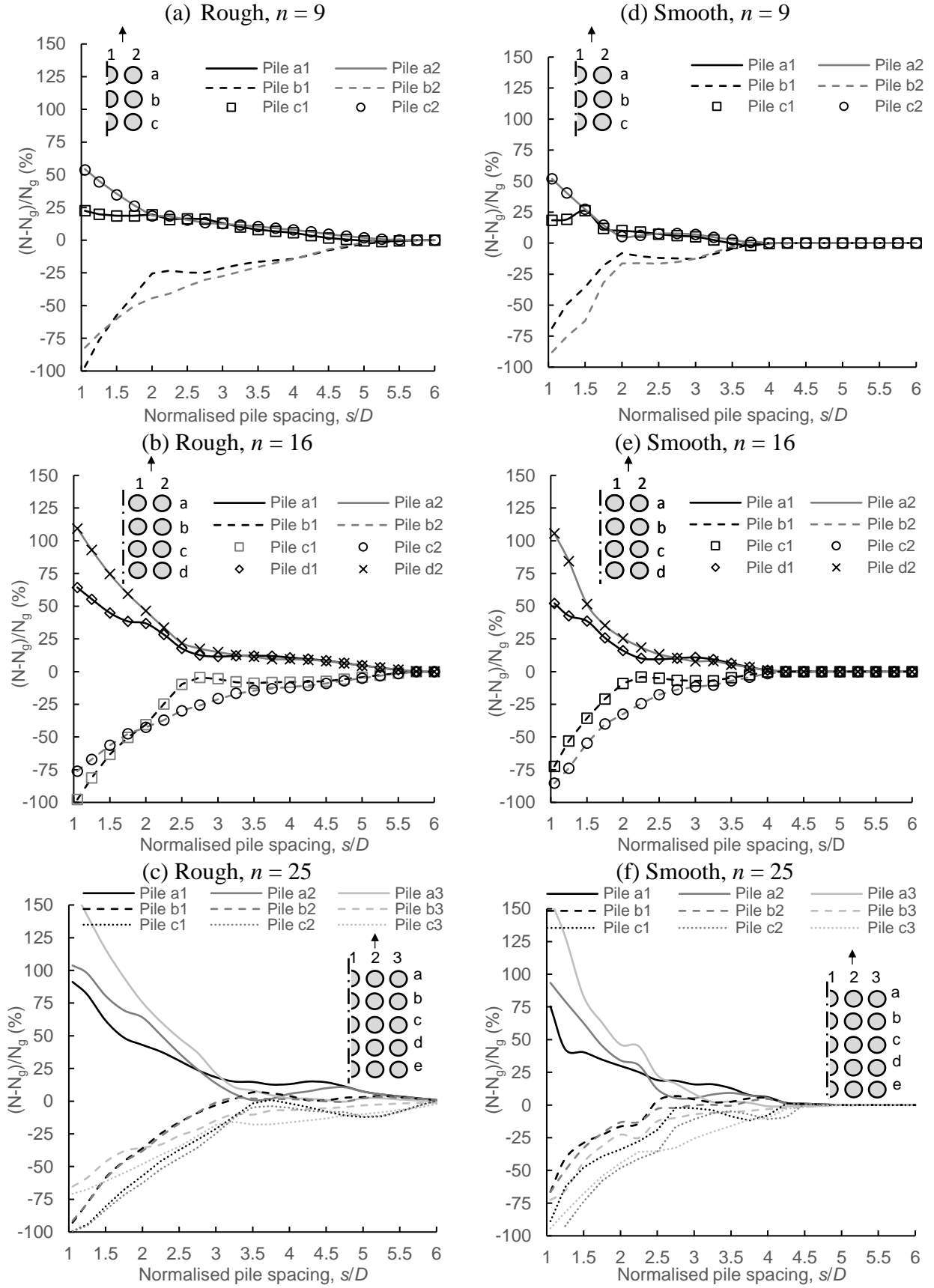


**Fig. 9** FE-predicted influence of  $s/D$  on pile group load-sharing for group sizes of 9, 16 and 25 piles and both smooth and rough interfaces. The location of each pile is shown in the corresponding schematic of the pile group superimposed on each figure.

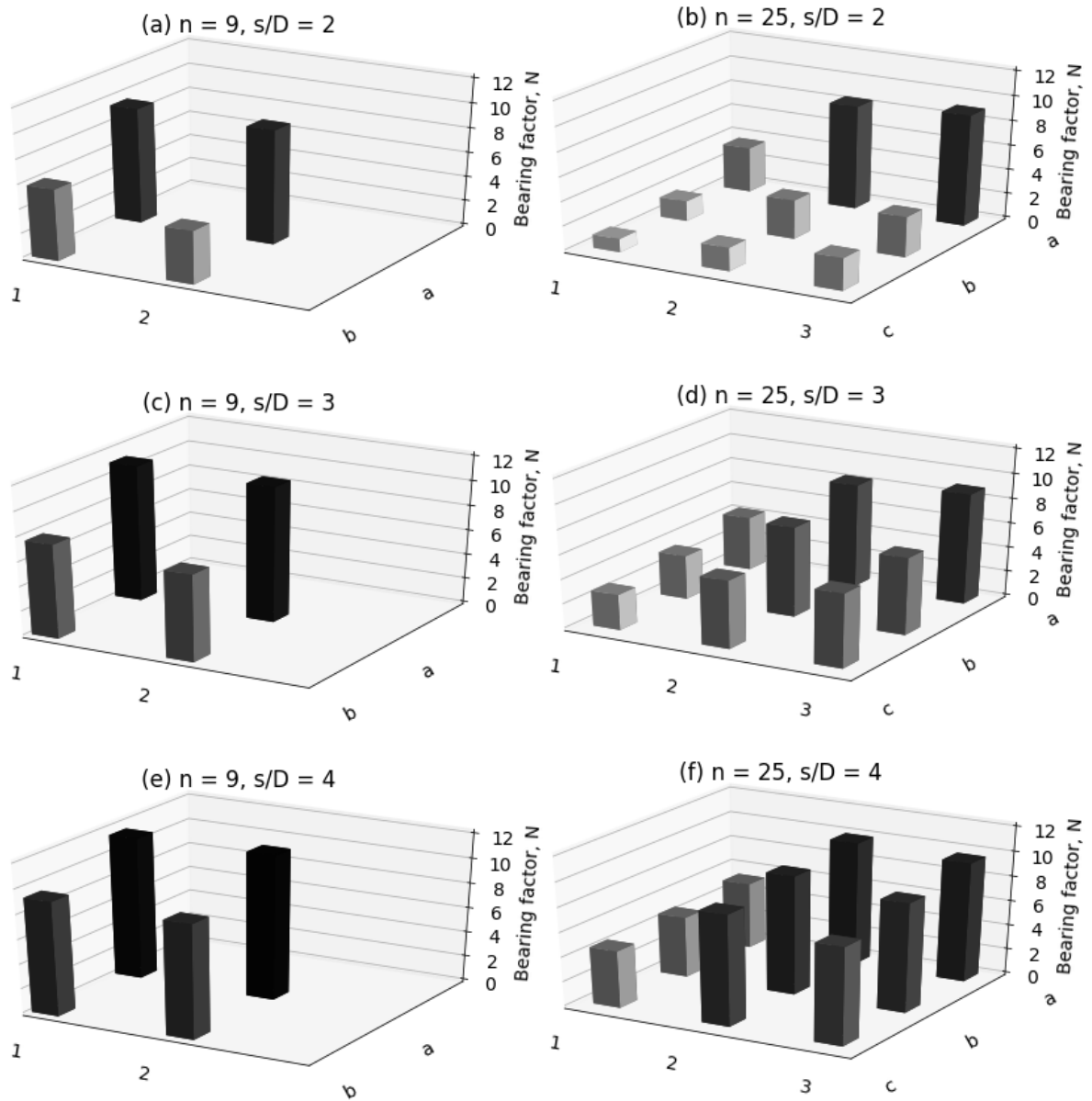


**Fig. 10** Load distributions within  $n = 9$  and  $n = 25$  pile groups for a rough pile-soil interface.

Axis labels denote pile positions according to Fig. 9

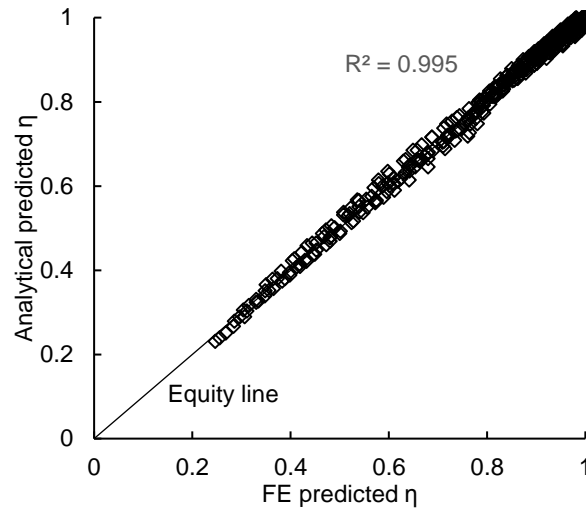


**Fig. 11** Comparison between analytical predictions of  $\eta$  and finite element results

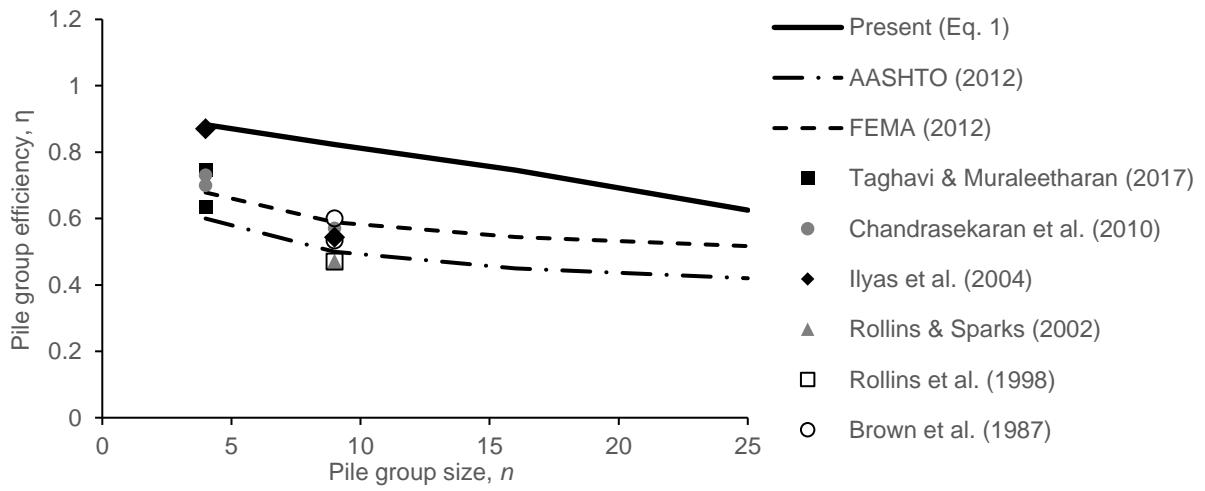


**Fig. 12** Comparison between present analytical predictions, previously-documented field data and predictions using existing design guidelines;  $s/D = 3$ ,  $\alpha = 1$